

ELR-Negative CXC Chemokine CXCL11 (IP-9/I-TAC) Facilitates Dermal and Epidermal Maturation during Wound Repair

Cecelia C. Yates,^{*†} Diana Whaley,^{*} Amy Y-Chen,^{*} Priya Kulesekaran,^{*} Patricia A. Hebda,[‡] and Alan Wells^{*†}

From the Departments of Pathology^{*} and Otolaryngology,[‡] University of Pittsburgh and Pittsburgh Veteran's Administration Medical Center, Pittsburgh, Pennsylvania; and the Carver Research Foundation,[†] Tuskegee University, Tuskegee, Alabama

In skin wounds, the chemokine CXCR3 receptor appears to play a key role in coordinating the switch from regeneration of the ontogenically distinct mesenchymal and epithelial compartments toward maturation. However, because CXCR3 equivalently binds four different ELR-devoid CXC chemokines (ie, PF4/CXCL4, IP-10/CXCL10, MIG/CXCL9, and IP-9/CXCL11), we sought to identify the ligand that coordinates epidermal coverage with the maturation of the underlying superficial dermis. Because CXCL11 (IP-9 or I-TAC) is produced by redifferentiating keratinocytes late in the regenerative phase when re-epithelialization is completed and matrix maturation ensues, we generated mice in which an antisense construct (IP-9AS) eliminated IP-9 expression during the wound-healing process. Both full and partial thickness excisional wounds were created and analyzed histologically throughout a 2-month period. Wound healing was impaired in the IP-9AS mice, with a hypercellular and immature dermis noted even after 60 days. Re-epithelialization was delayed with a deficient delineating basement membrane persisting in mice expressing the IP-9AS construct. Provisional matrix components persisted in the dermis, and the mature basement membrane components laminin V and collagen IV were severely diminished. Interestingly, the inflammatory response was not diminished despite IP-9/I-TAC being chemotactic for such cells. We conclude that IP-9 is a key ligand in the CXCR3 signaling system for wound repair, promoting re-epithelialization and modulating the maturation of the

superficial dermis. (Am J Pathol 2008, 173:643–652; DOI: 10.2353/ajpath.2008.070990)

Skin wound healing is remarkable for a biphasic cellular process that entails an initial hypercellular phase with a provisional, undifferentiated matrix followed by loss of many of the initial cells and structures concomitant with significant turnover resulting in maturation of the extracellular matrix. A key question remains as to which signal(s) dictates this switch. Recent findings have suggested key factors for both vascular involution^{1,2} and dermal regression/maturation.² However, a key requirement for any wound maturation signal is that it would coordinate responses between the ontologically distinct epidermal and dermal compartments. Thus, the onset of dermal maturation must coincide with successful re-epithelialization, otherwise the wound will be prone to dehiscence or chronicity.

Our recent findings suggest that this paracrine epithelial-mesenchymal loop is mediated at least in part by ligands for the CXCR3 chemokine receptor. This seven transmembrane classical G-protein-coupled receptor has two isoforms, with the b isoform predominant on adherent cells as opposed to the form on the hematopoietic lineages.³ This CXCR3b binds, seemingly interchangeably, CXC chemokines that lack the ELR (aspartic acid, leucine, and arginine) motif. In addition to functioning in other physiological and pathological processes, all four chemokines appear during wound healing. CXCL4 (PF4) is released by platelets during the initial hemostatic phase,⁴ with CXCL9 (Mig) being produced during the early inflammatory response.⁵ The other two ELR-nega-

Supported by the National Institutes of Health (National Institute of General Medical Science grant GM063569) and the Pittsburgh Veterans Administration Medical Center.

Accepted for publication June 2, 2008.

Current address of A.Y.: Wayne State University, Detroit, MI; and P.K.: University of Michigan, Ann Arbor, MI.

Address reprint requests to Alan Wells, M.D., D.M.Sc., University of Pittsburgh, Department of Pathology, 3550 Terrace St., Scaife Hall, S-713, Pittsburgh, PA 15261. E-mail: wellsa@upmc.edu.

tive CXC chemokines are more intriguing because they appear in the later regenerative phase seemingly preceding the maturation switch. CXCL10 (IP-10) is produced deep in the dermis by the neovascular endothelial cells and in the epidermis.^{2,6} IP-9 derives from the redifferentiating keratinocytes just behind the leading tongue of re-epithelializing keratinocytes.^{2,7}

What directs us to hypothesize that these two later factors, IP-10 and IP-9, are critical to wound maturation is not only the timing of appearance but the effects of CXCR3 signaling. CXCR3 activation limits the motility induced by classical growth factors of fibroblasts and endothelial cells.⁷⁻⁹ The effect on fibroblasts is to channel the growth factor-induced transcellular contractility to maturation-related matrix compaction.¹⁰ Furthermore, not only is CXCR3 signaling angiostatic,^{9,11} but its activation of μ -calpain (calpain I) leads to vascular disintegration through anoikis (R. Bodnar, manuscript submitted). Importantly, CXCR3 signaling is not inhibitory to dedifferentiated keratinocytes but actually stimulates motility, being additive with growth factors.^{7,12} Thus, we hypothesized that IP-9 is a key integrator of epidermal and dermal responses, by driving speedy re-epithelialization of the wound simultaneous with directing maturation and strengthening of the dermal wound bed.² To test this, we have prevented IP-9 expression in keratinocytes during wound repair, by generating transgenic mice in which an antisense construct is driven from the basal keratinocyte-specific cytokeratin K5 promoter.¹³

Materials and Methods

Animals

FVB mice were used throughout. The antisense construct was generated by cloning the IP-9 cDNA into the *Sna*B1 site of the pBK5 vector, which contains 5.2 kb of the bovine cytokeratin K5 promoter (a kind gift from Dr. Jose Jorcano, CIEMAT, Madrid, Spain).¹³ After verification that this construct could significantly blunt the interferon- γ induction of IP-9 in human keratinocytes (Figure 1A) this was used to generate transgenic mice in the University of Pennsylvania (Philadelphia, PA) transgenic core facility. Founders were identified by germline transmission of the transgene using polymerase chain reaction of tail clip DNA (forward: 5'-CATATGAAGTCCTGGAAAAGGG-3'; reverse: 5'-ACAACACTACACCCTGGTCATCA-3'). Mice were sib-mated by transgene \times wild type. The transgenic mice are referred to as IP-9AS. In the transgene, IP-9 production was not noted during wound repair (Figure 1B).

All studies on these animals were performed in compliance with the Institutional Animal Care and Use Committees of the Veteran's Administration and University of Pittsburgh. These animals were housed in a facility of Veteran's Affairs Medical Center, Pittsburgh, PA, accredited by the Association for the Assessment and Accreditation of Laboratory Animal Care. Serological analyses did not detect blood-borne pathogens or evidence of infection. Mice were housed in individual cages after wounding and maintained under a 12-hour light/dark cy-

cle and temperature in accordance with the guidelines approved by the Institutional Animal Care and Use Committee.

Wounding

Male and female mice (7 to 8 weeks of age weighing ~25 g) were anesthetized with an intraperitoneal injection containing ketamine (75 mg/kg) and xylazine (5 mg/kg). The backs were cleaned, shaved, and sterilized with betadine solution. For full thickness wounds, a 2-cm full-thickness wound through the epidermis and dermis was made on one side of the dorsal midline, using sharp scissors, with the contralateral uninjured skin serving as a control. Partial-thickness wounds were made with a specially-modified dermatome.¹⁴ The wounds were covered with liquid occlusive dressing (New-Skin; Medtech, Jackson, WY). This experiment was performed in duplicate.

To follow the wound progression visually, the animals were lightly anesthetized for several seconds with a halothane cone. A transparent sheet was placed over the wound. Re-epithelialization of the wound was traced at 2-day intervals until complete closure. These parameters were compared between the wild-type and IP-9AS. The tracings were measured using Adobe Photoshop image analysis software (version 7.0; Adobe System Inc., San Jose, CA).

Histological Analyses

Wound bed biopsies, including a margin of nonwounded skin, were collected at days 5, 7, 14, 21, 30, and 60 after wounding. Wound biopsies were fixed in 10% buffered formalin, processed, and embedded in paraffin blocks using standard protocols. Four- μ m tissue sections were stained with hematoxylin and eosin (H&E) for assessment of general tissue and cellular morphology. Collagen deposition, content, and alignment were evaluated by Masson's Trichrome and Picrosirius Red staining. Slides were quantitatively analyzed using MetaMorph (Universal Imaging Corp., Molecular Devices, West Chester, PA). The histological scoring system was developed based on the scoring system by Greenhalgh.¹⁵ Most of the scoring systems use more than one determinant to assess the histological parameters, as briefly described below.

Inflammation

Acute inflammation was defined as the presence of neutrophils and chronic inflammation by the presence of plasma and monocytic cells (0, none; 1, slight; 2, moderate; 3, abundant). In both situations the scale was secondary to relative level of cells per high-power field.

Epidermal and Dermal Maturation

Histopathological examination of mouse tissues was performed blinded by a trained histopathologist. Qualitative

assessments were made concerning aspects of dermal and epidermal maturation, inflammation, and granulation tissue. The samples were scored on a scale of 0 to 4 for epidermal healing (0, no migration; 1, partial migration; 2, complete migration with partial keratinization; 3, complete keratinization; and 4, normal epidermis) and dermal healing (0, no healing; 1, inflammatory infiltrate; 2, granulation tissue present—fibroplasias and angiogenesis; 3, collagen deposition replacing granulation tissue >50%; and 4, complete healing).

Collagen Content

Masson's trichrome staining was used to assess collagen content as previously described by Yates and colleagues.² Collagen content was assessed using Meta-Morph analysis (Molecular Devices, Sunnyvale, CA). Stained wound biopsies were compared with that of the unwounded controls: at all times the colors was maintained to compare the blue- and red-stained areas. The final output was integrated intensity based on total area and staining intensity at individual pixels. All wound biopsies were stained at the same time to eliminate staining variation.

Collagen Alignment and Organization

Picrosirius Red staining was used to assess alignment and organization in intact biopsies. Briefly, picric acid (Sigma-Aldrich, St. Louis, MO) was dissolved in 500 ml of distilled water. To this, 0.1 g of Sirius Red F3BA was added per 100 ml (Sigma-Aldrich). Paraffin-embedded tissue sections were rehydrated and stained with picric acid. Collagen fibrils were then evaluated by means of polarized light microscopy for both collagen fibril thickness and coherence alignment. Polarization microscopy reveals closely packed thick fibrils of type I collagen fibers as either red-orange intense birefringence in the hypertrophic tissue, with thin short loose fibrils as yellow-green. Distribution of fibrils in terms of thickness (cross-sectional area) and arrangement in terms of length of the collagen scars were quantitatively analyzed using Meta-Morph (Molecular Devices). Biopsies of unwounded skin served to set the threshold against which the wound biopsies were measured. Percent staining of mature fibers was determined by comparing the total staining intensity of the birefringence (area of staining summed for intensity of pixel) of wound biopsies compared with the biopsies of the contralateral unwounded skin.²

Immunohistochemistry

Sections for immunohistochemical analysis were incubated with appropriately diluted primary antibody, after antigen retrieval. Antigen staining was performed using diaminobenzidine (Vector Laboratories, Burlingame, CA), then counterstained with Mayer's hematoxylin and coverslipped. In all cases, secondary antibody alone served as

a negative control, with various tissues serving as positive controls.

Paraffin sections of 4 to 5 μm were prepared for antibody staining. The following antibodies were used for immunohistochemical staining for mouse: fibronectin (rabbit polyclonal; Rockland, Inc., Gilbertsville, PA), IP-9 (goat polyclonal; Santa Cruz Biotechnology, Santa Cruz, CA), tenascin-C (rat polyclonal; R&D Systems, Minneapolis, MN), collagen IV (rabbit polyclonal; Abcam Inc., Cambridge, MA), and Ki-67 (rabbit polyclonal, Abcam Inc.).

Tensile Strength

Biopsies were wrapped flat in foil, snap-frozen in liquid nitrogen, and then stored at -80°C . For the tensile strength measurements, the frozen specimens were divided into two samples, the cross-sectional area measured with calipers, and then the samples were clamped in a tensiometer and force-exerted until wound disruption, as previously described.¹⁴ The tensiometer was calibrated after every third sample with a wide range of weights. Measurements were recorded by a customized computer software program and tensile strength calculated using the formula: maximum tensiometer reading (converted to g) divided by cross-sectional area (mm^2) = tensile strength (g/mm^2). The results for individual specimens from one wound were combined to determine an average tensile strength per wound. The average tensile strength per wound was tabulated for each group at days 7, 14, 21, 30, and 60 after wounding.

In Situ Hybridization

Pspt 18 plasmid (Roche Molecular Diagnostics, Indianapolis, IN) harboring the IP-9 sequence⁹ in either orientation were linearized and Digoxigenin DIG labeled. Sense (control) and anti-sense RNA probes were obtained by using the DIG labeling RNA kit (Roche Molecular Diagnostics, Indianapolis, IN) with SP6 RNA polymerase. Labeled probes were purified by the Qiagen (Valencia, CA) spin column kit. *In situ* hybridization was performed on formalin-fixed, paraffin-embedded wound biopsy sections from different days as described previously. These were overlaid with 100 μl of hybridization buffer containing 100 ng of probe and incubated overnight at 37°C in a humidified chamber. After hybridization, nonhybridized probe were removed using high stringency washes. The sections were incubated with anti-DIG-labeled secondary antibody conjugated with alkaline phosphatase. Staining reaction was performed using BCIP/NBT substrate and photographed.

Statistical Analysis

Results are expressed as mean \pm SD. Statistical differences between groups were determined by the 2 tailed Student's *t*-test. Paired analyses were performed be-

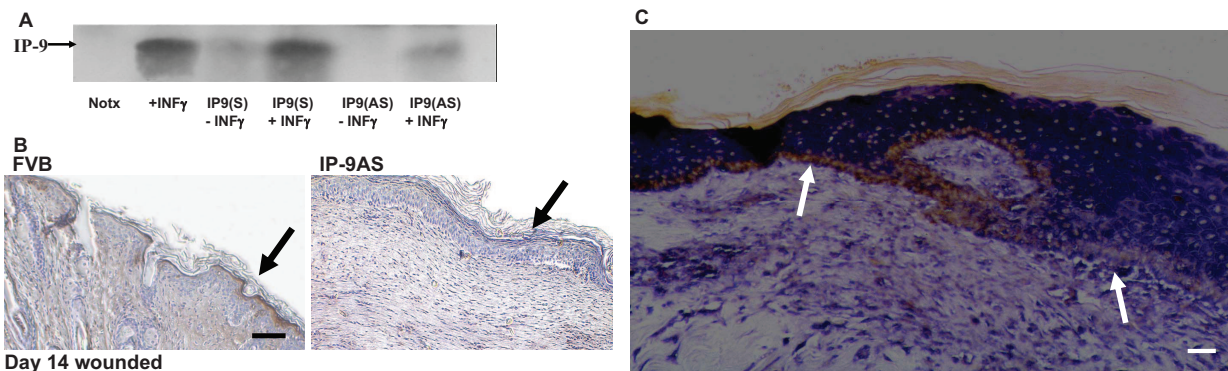


Figure 1. A: To verify that the pBK5-IPAS construct could block interferon- γ induction of IP-9, pBK5-IPAS was transfected into human keratinocytes (HeK293) and stimulated with interferon- γ . Immunoblot analysis (using equal protein loading) revealed IP-9 is not expressed in keratinocytes transfected with the pBK5-IPAS construct after interferon- γ induction. Notch, diluent alone. **B:** Immunohistochemistry demonstrated IP-9 suppression in the IP-9AS mice biopsies from day 14 of an experimental excisional wound. Presence of IP-9 is seen in the basal layer of keratinocytes that express keratin K5/K8 in the FVB mice (arrows). **C:** Characterization of IP-9 mRNA expression in wound biopsies on day 14 is visualized by *in situ* hybridization with DIG-labeled anti-sense RNA probes. Sense probes did not demonstrate any staining (data not shown). Significant staining was noted in the basal keratinocytes back from the margin of wound bed (WB) (transition to mesenchymal keratinocytes). Shown is the graded decrease in IP-9 mRNA expression from the differentiated basal keratinocytes to the re-epithelializing keratinocytes (arrows). No staining is noted in unwounded skin (data not shown). Shown are representative of at least three experiments. Scale bars: 100 μ m (B); 50 μ m (C). Original magnifications: \times 200 (B); \times 400 (C).

tween all groups. Comparisons throughout time were performed by analysis of variance. Significance is deemed at $P < 0.05$.

Results

Lack of IP-9 Production Delays Wound Coverage

Keratinocytes produce IP-9 in response to wounding both *in vitro* and *in vivo*.^{2,7} IP-9 mRNA is detectable just behind the leading edge of the wound (Figure 1C). Protein is noted in murine wounds as early as day 4 and expression persists as late as day 16.² Because IP-9 expression during wound repair appears mainly limited to the dedifferentiated keratinocytes of the epidermis we sought to specifically ablate

such production in mice using a promoter that is highly active in the dedifferentiated keratinocytes, the cytokeratin K5 promoter (Figure 1B).¹⁶

The pathophysiological effects of the suppression of IP-9 during healing were determined by creating full and partial thickness excisional wounds in the dorsal skin on the IP-9AS and FVB (wild type) mice. Grossly in partial thickness wounds, a delay in healing was observed in the IP-9AS mice with the eschar being present at least 14 days longer than in the wild-type mice (Figure 2). In the full thickness wounds, the gross deficits were more subtle (data not shown). This was not unexpected because full thickness skin wounds in rodents close mainly by contraction¹⁵; furthermore, deep in the dermis, CXCL10/IP-10 appears to be the predominant CXCR3 ligand.^{2,17}

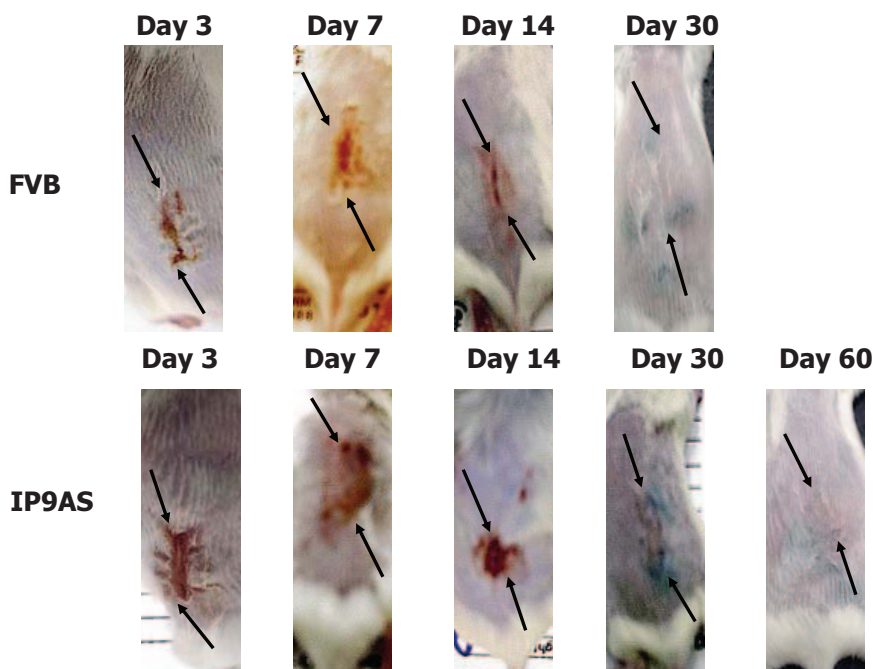


Figure 2. Representative photographs are shown of partial thickness wounds created with a specially-modified dermatome at various days up to day 60. IP-9AS wound eschar remained up to 14 days longer than that of the FVB. As late as day 30 the IP-9AS wound showed abnormal healing of a scab whereas the FVB wound was completely healed. Representative of six mice at each condition/time point. The black marks are from India ink used to delineate the original wound (arrows show dorsal/caudal ends of wounds).

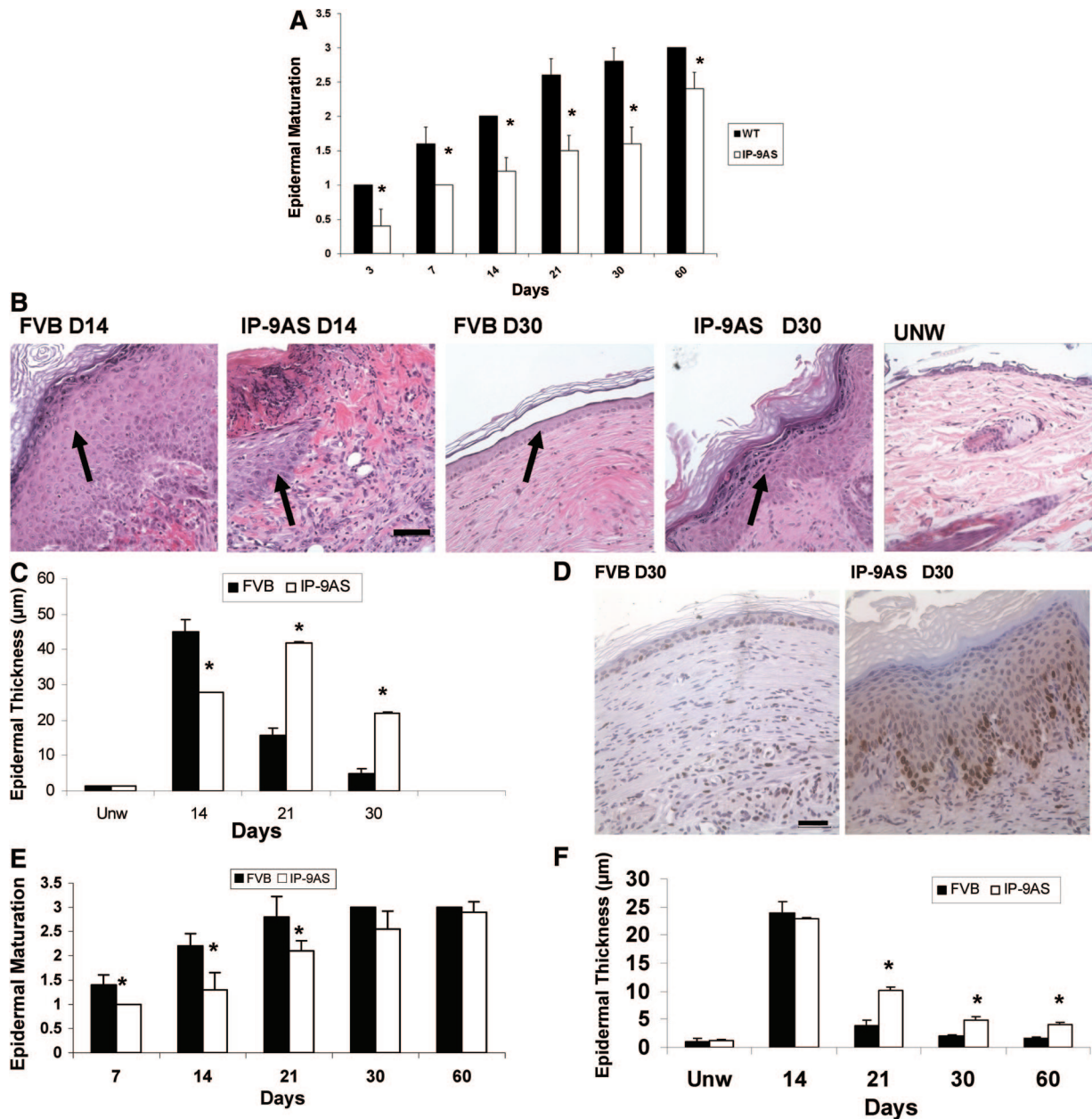


Figure 3. A: Partial thickness wounds $\sim 7 \times 10$ mm and 0.2 to 0.3 mm deep were made on the skin of each animal with a dermatome. Epidermal maturation, determined by examination of histology, showed a delay in IP-9AS wounds as late as day 60. B: Representative H&E-stained sections reveal a hindrance in maturation in IP-9AS wounds and a thicker hyperproliferative epidermal layer (arrows point to the epidermis in the healing wound bed). These wounds approach but do not reach the state noted in unwounded skin (UNW). C: Quantitative measurements of epidermal cell layers shows IP-9AS mice partial thickness wounds to be significantly thicker as late as 30 days after wounding in comparison to FVB mice. Unw, unwounded. D: Proliferation marker (Ki-67 staining) indicated the IP-9AS wounds contained proliferating keratinocytes 30 days after wounding suggesting active remodeling epidermis whereas the FVB mice resembled resting state as in normal skin. E: Epidermal maturation of 2-cm full-thickness wounds of IP-9AS mice proceeded at a slightly delayed rate in comparison to FVB mice. F: Quantitative measurements of epidermal cell layers shows IP-9AS mice full-thickness wounds to be significantly thicker as late as 30 days after wounding in comparison to FVB mice. In A and C shown are mean \pm SD ($n = 6$, $*P < 0.05$; where no error bars are noted, they are subsumed within the bar); others are representative of six mice. Scale bars = 50 μ m. Original magnifications, $\times 400$.

Normal Re-Epithelialization Depends on IP-9 Production

Analyzed histologically, the wounds in the IP-9AS mice showed both a delayed re-epithelialization and an immature epidermis. In partial thickness wounds, the progressing keratinocyte tongue was delayed (Figure 3A), and even where the underlying dermis was covered, the epidermal layer was thicker (Figure 3B) with more

transit-amplifying cells even as long as 30 days after wounding at which time the wounds in wild-type mice appear fully healed. Even in the wild-type mice, the wounds at 30 days are not similar to unwounded skin, although they do demonstrate significant wound maturation; this level of maturation is significantly less in the wounds in the IP-9AS mice. This correlates with the corresponding increase in the number of cell layers that constitute the epidermis in the IP-9AS wounds

(0.0202 mm in IP-9AS versus 0.0080 mm in the FVB mice) (Figure 3C).

The late-stage wounds in the wild-type mice resemble that of normal skin with a low number of keratinocytes presenting the proliferation marker Ki-67, whereas a greater number of nuclei stain positive for Ki-67 as late as 30 days after injury in the IP-9AS mice (Figure 3D) suggesting a degree of wound retardation or immaturity in these mice. Epidermal maturation is also deficient in the full-thickness wounds (Figure 3E), showing that this maturation aspect is independent of actual wound edge juxtapositioning. The number of cell layers also increased in IP-9AS full-thickness wounds (Figure 3F).

Dermal Healing Is Limited in the Suppression of IP-9 Signaling

Fibroplasia and epithelialization are two distant aspects of the skin healing, both of which appear impacted by CXCR3 signaling.² It has been speculated that keratinocyte-derived soluble factors signal the maturation of the underlying dermis to synchronize the wound repair.¹⁸ Even in full thickness wounds, dermal maturation was delayed up to 60 days after wounding (Figure 4A). Masson trichrome staining for collagen content shows a clear morphological difference in the dermal matrix with the wounds in IP-9AS mice having less deposited collagen and greater fibroblast cellularity in comparison to wounds in FVB control mice (Figure 4, B and C). Quantification of the dermal wounds revealed that IP-9AS mice failed to properly remodel the dermal matrix as late as day 60 after wounding; Picrosirius Red staining showed that the IP-9AS wounds had shorter and less well connected collagen fibers resulting in a less well organized with respect to regain of tensile strength and immature scar (Figure 4, D and E). Consistent with the collagen immaturity, provisional matrix components including tenascin C and fibronectin are not present at day 21 (tenascin C) and day 14 (fibronectin) in the wounds of IP-9AS mice in comparison to wild type (Figure 4F).

Because it is well documented that tensile properties of a wound depend not only on the amount of collagen, but also on the organization and crosslinking of the matrix we assessed the biomechanical properties of the wounds. Tensiometry demonstrated that IP-9AS mice wounds lagged behind those of the control mice with respect to regain of tensile strength; even at 60 days after wounding, the IP-9AS mice regained only 60 to 65% of the prewounding strength compared to the 75 to 80% for the control mice (Figure 4G). These results suggest that not only does chemokine IP-9 affect epidermal healing but dermal healing as well by contributing to fibroblast immigration, collagen bundling and alignment, and dermal strength (collagen organization).

In the partial thickness wounds, the superficial, papillary dermis was removed by the dermatome.¹⁴ In this region, dermal repair was deficient in IP-9AS wounds, showing collagen and matrix immaturity. Importantly for skin healing, the delineating basement membrane between the dermal and epidermal compartments was de-

ficient. Most obvious, is the elevated expression of collagen IV (Figure 5) in the late healing phase of the IP-9AS mice suggesting that the epidermis-dermal junction has yet to properly form, resulting in a looser connection between these layers in the healed wounds of the IP-9AS mice (Figure 3B).

The Inflammatory Response Appears to Be Unaffected by IP-9 Ablation

The first aspect of wound healing after hemostasis involves an inflammatory response with a rapid infiltration of polymorphonuclear leukocytes (acute response) followed by macrophages and lymphocytes (chronic response). This is thought to be crucial to re-establishing the microbial barrier function of the skin. Interestingly, although CXCR3 ligands limit migration of stromal and endothelial cells, they are chemotactic for hematopoietic cells.¹⁹ As such it was critical to determine whether the lack of the epidermally-derived IP-9 blunted this response. Unexpectedly, the presence of polymorphonuclear (Figure 6A) and mononuclear (Figure 6B) leukocytes was similar in wounds of both FVB and IP-9AS mice when determined by histopathological analyses. Thus, the differences in dermal and epidermal maturation noted above were not because of differences in the early inflammatory infiltrations.

Discussion

Skin wound healing is a highly orchestrated process that results in the replacement of the tissue with structures derived from multiple lineages and even embryonic layers. Coordination between these distinct layers of epidermis and dermis is key to this neo-organogenesis. Soluble factors have been proposed as the communicators to synchronize the wound response, particularly during the later organ maturation phases.¹⁸ We have recently found that signaling through the CXCR3 receptor plays a major role in wound resolution, with an immature and hypercellular skin persisting in the suppression of such signaling.² The receptor side comprises only half of the equation because CXCR3 is the sole defined receptor for four genetically distinct ligands—CXCL4 (PF4), CXCL9 (MIG), CXCL10 (IP-10), and CXCL11 (IP-9 or I-TAC).²⁰ Although PF4 is released by platelets during clotting⁴ and MIG is expressed by the inflammatory cells that infiltrate a wound,²¹ the latter two ligands appear coincident with wound maturation.^{2,7} Of these two, IP-9 is more restricted in being derived predominantly from keratinocytes that appear to have undergone redifferentiation after covering the regenerative dermis; IP-10 appears to be produced by multiple cell types throughout the wound. As such, we postulated that IP-9 is key to communicating the epidermal maturation status to the underlying wound dermis.

Our model postulated that suppression of IP-9 expression would result in delayed wound maturation, particularly in the epidermal and superficial dermal compartments, similar to that noted in wounds in the CXCR3-devoid animals.²

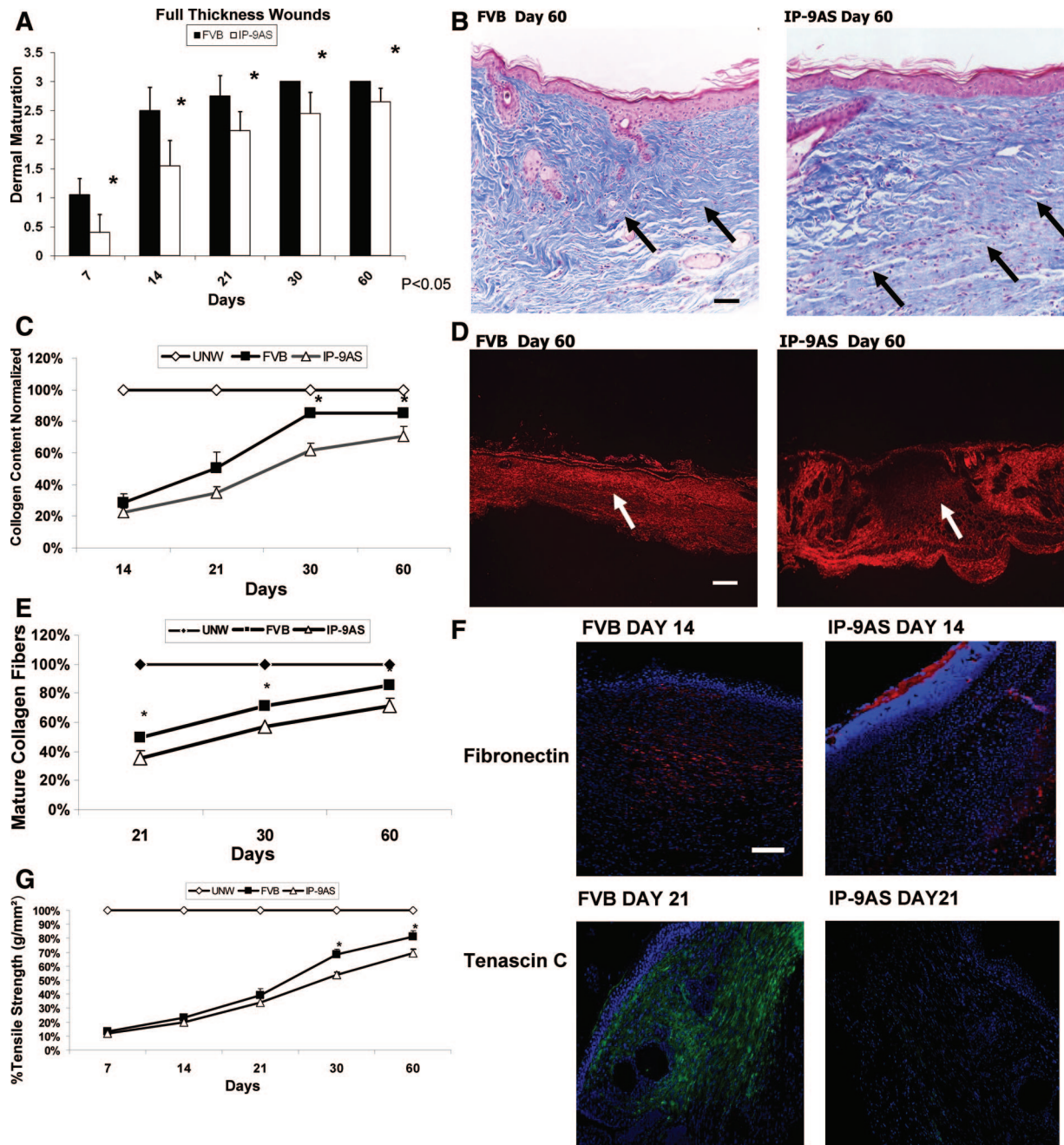


Figure 4. A: Full-thickness wounds with surrounding normal skin were biopsied from the IP-9AS and FVB mice at day 7 to 60 after wounding. B: Masson Trichrome microscopic images showed distinguishable patterns of collagen remodeling between the IP-9AS and FVB mice 60 days after wounding. C: New collagen synthesis was quantitatively measured and revealed that healing of wounds in IP-9AS mice resulted in significantly less collagen than those in FVB mice throughout the healing process. Unw, unwounded. D: Picosirius Red staining showing that the IP-9AS wounds were less organized and aligned with an immature scar and shorter collagen fibers. Shown are representative photomicrographs of entire wound. E: Quantification of the Picosirius Red stain showed a significant difference between the wound healing in IP-9AS and FVB mice throughout the healing process. Quantification performed on higher power photomicrographs. F: Interestingly, wound immaturity corresponds with a stain of fibronectin (red) and tenascin C (green) that appears to be delayed in the IP-9AS mice; nuclei are stained by DAPI stain (blue). G: Tensile strength measurement of full-thickness wounds. IP-9AS wounds showed significantly less tensile strength than the FVB wounds as late as day 60 after wounding. In A, C, E, and G shown are mean \pm SD ($n = 6$, $*P < 0.05$); others are representative of six mice. The arrows refer to areas in the wound bed with which to best appreciate the differences between the mice. Scale bars: 50 μ m (B); 200 μ m (D); 100 μ m (F). Original magnifications: $\times 400$ (B, E); $\times 100$ (D); $\times 200$ (F).

We abrogated IP-9 production in mice by expressing an antisense construct from the cytokeratin K5 promoter that is active in proliferative basal keratinocytes,^{22,23} the cells that transcribe the IP-9 gene. This resulted in a mouse in which IP-9 production was absent from skin wounds. Wounding of these mice resulted in a persistent hyper-

cellular wound and delayed maturation of the compartments similar to that seen in wounds in the CXCR3-devoid mice. These findings are consistent with the underlying molecular mechanisms whereby CXCR3 signaling i) limits fibroblast and endothelial cell motility by preventing μ -calpain activation by mitogenic growth fac-

Collagen IV

FVB DAY 21

IP-9AS Day 21

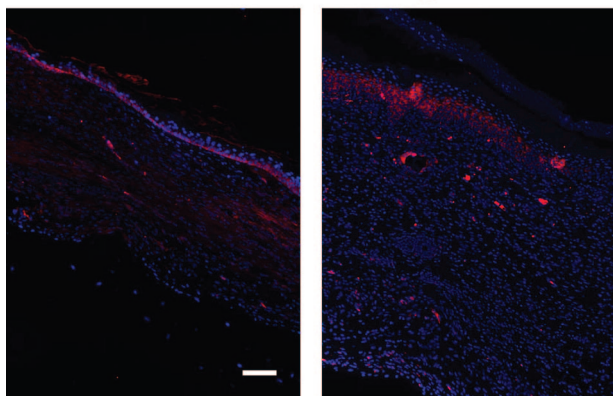


Figure 5. Collagen IV in IP-9AS mice at 21 days after wounding exhibits increased expression suggesting an immature proliferating and remodeling epidermis-dermal junction whereas FVB mice resembled a quiescent epidermis basement membrane late in the healing phase. Shown are from one of three mice. Scale bar = 100 μ m. Original magnifications, $\times 200$.

tors such as EGF, PDGF, and VEGF^{8,9,24}; ii) channels wound bed signals toward matrix contraction and reorganization by fibroblasts^{10,25}; and iii) induces endothelial cell apoptosis via a μ -calpain-mediated process (R. Bodnar, manuscript submitted). The absence of these stop immigration and involution, at least for endothelial cells, and maturation, at least for fibroblasts, signals should result in hypercellular wounds with persistent expression of provisional matrix components, as is noted. Contrarily, we also had found that CXCR3 signaling promotes keratinocyte motility and coverage of a monolayer gap by μ -calpain activation reducing adhesiveness to shift these cells toward a more favorable regime for motility.^{7,12} We

found that re-epithelialization appeared delayed even in these full-thickness wounds. However, full-thickness wounds in rodents close primarily by contraction because the skin is only loosely connected to the underlying integumen in distinction to the human situation. For this reason, we created partial thickness wounds using a specially modified dermatome that removed the epidermis and only the superficial dermis.¹⁴ These wounds were re-epithelialized from the margins, in a situation more relevant to wound healing in humans. Examining these wounds, we found that re-epithelialization was somewhat delayed, consistent with IP-9 signaling motility, although to a less degree than classical growth factors present in the wound.⁷ What was more striking was the hypertrophic epidermis and the immaturity of the underlying basement membrane. This would imply that the IP-9/CXCR3 signaling axis, although being a minor player in keratinocyte migration, might play a major role in signaling the wound resolution stage. Whether the two aspects of epidermal cellularity and basement membrane construction are related, and if so, in which hierarchical status, remains to be determined in future studies that lie beyond the scope of the present communication.

An aspect of wound healing that has remained enigmatic despite extensive investigation is the initial exuberant inflammatory response. Intuitively such a response would be needed when the main barrier to external microbes is breached as in a skin wound. However, there is also evidence that such an inflammatory response, particularly if prolonged or exaggerated, leads to scarring; fetal wounds that regenerate lack this inflammatory response. Thus, a fine balance must be maintained between battling infection and limiting damage to the surrounding regenerating tissues. A number of factors are

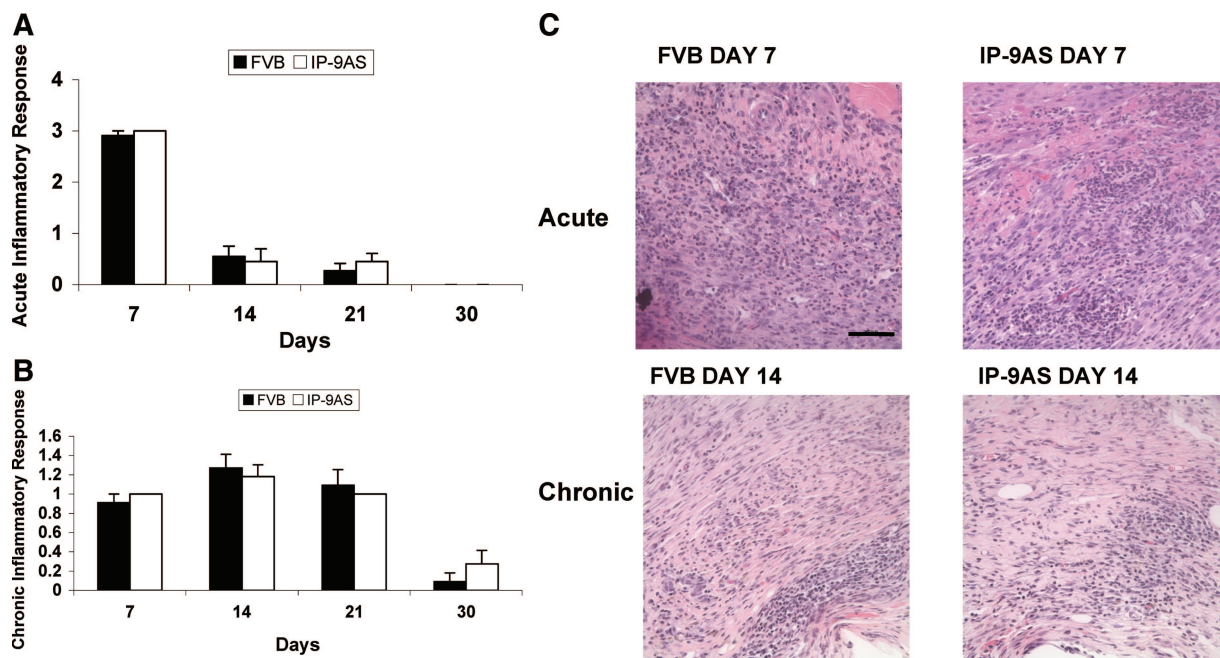


Figure 6. Histopathological analysis of the acute (A) and chronic (B) inflammatory responses determined that there was not a difference in macrophage or polymorphonuclear and mononuclear leukocyte infiltration in the wounds of IP-9AS and FVB mice. C: Representative H&E-stained sections showing acute inflammation at day 7 and chronic inflammation at day 14. Shown are mean \pm SD ($n = 6$, $*P < 0.05$). Scale bar = 50 μ m. Original magnifications, $\times 400$.

present immediately after wounding that attract the innate immune response first followed by the cells of the acquired immune response, among these the CXCR3 ligands are chemoattractants for these cells.²⁶ It is most likely that PF4 and MIG play a greater role in recruiting these cells because of their appearance much earlier in wound healing at times of greatest inflammatory response. However, there is still the open question of whether the lack of IP-9 production by keratinocytes would compromise the inflammatory response after the first week. We did not note a deficit in the inflammatory response at the crude level of histopathological analyses. In fact, in initial analyses of wounds in mice lacking CXCR3, and thus eliminating the signals from PF4 and MIG also, we do not see a difference in the histology of the inflammatory response (data not shown). This would imply that many other factors, not limited to the other CXCR3 ligands, regulate the important function of preventing wound contamination and infection. However, it must be noted that these wounds were created under clean conditions in which the inflammatory response is not stressed; contaminated wounds might show much greater differences in healing outcomes in the suppression of IP-9 or more importantly all CXCR3 signaling. Furthermore, because IP-9 is up-regulated during dermal immune disorders,²⁷ the relationship between this chemokine and acquired immunity awaits further investigation.

Herein, are presented data that implicate IP-9 as a key communicator between the epidermis and dermis to regulate wound maturation during the late regenerative and resolution phases of healing. The similarity of wounds in mice lacking just IP-9 production by keratinocytes to those in mice in which all CXCR3 signaling is absent because of gene deletion,^{2,28} suggests that IP-9 is the main chemokine for wound maturation. This would imply that premature IP-9 expression or exogenous addition might arrest wound healing. In usual circumstances this would lead to adverse conditions of weak wounds prone to ulceration. However, there are situations one could envision that would limit scarring or slow healing to allow sequential reconstruction.

Acknowledgments

We thank Dr. Richard Bodnar, Diane George, Dr. Joseph Newsome, Dr. Shveta Hood, and Dr. Latha Satish for providing suggestions and discussions; and Dr. Jose Jorcano (CIEMAT, Madrid, Spain) for kindly providing the K5 expression vector.

References

1. Rosenkilde MM, Schwartz TW: The chemokine system—a major regulator of angiogenesis in health and disease. *APMIS* 2004, 112:481–495
2. Yates CC, Whaley D, Kulasekaran P, Hancock WW, Lu B, Bodnar R, Newsome J, Hebda PA, Wells A: Delayed and deficient dermal maturation in mice lacking the CXCR3 ELR-negative CXC chemokine receptor. *Am J Pathol* 2007, 171:484–495

3. Lasagni L, Francalanci M, Annunziato F, Lazzeri E, Giannini S, Cosmi L, Sagrinati C, Mazzinghi B, Orlando C, Maggi E, Marra F, Romagnani S, Serio M, Romagnani P: An alternatively spliced variant of CXCR3 mediates the inhibition of endothelial cell growth induced by IP-10, Mig, and I-TAC and acts as functional receptor for platelet factor 4. *J Exp Med* 2003, 197:1537–1549
4. Yamamoto T, Chikugo T, Tanaka Y: Elevated plasma levels of β -thromboglobulin and platelet factor 4 in patients with rheumatic disorders and cutaneous vasculitis. *Clin Rheumatol* 2002, 21: 501–504
5. Engelhardt E, Toksoy A, Goebeler M, Debus S, Brocker EB, Gillitzer R: Chemokines IL-8, GRO α , MCP-1, IP-10, and Mig are sequentially and differentially expressed during phase-specific infiltration of leukocyte subsets in human wound healing. *Am J Pathol* 1998, 153:1849–1860
6. Tensen CP, Flier J, vanderRaaij-Helmer EM, Sampat-Sardjoepersad S, vanderSchors RC, Leurs R, Scheper RJ, Boorsma DM, Willemze R: Human IP-9: a keratinocyte-derived high affinity CXC-chemokine ligand for the IP-10/Mig receptor (CXCR3). *J Invest Dermatol* 1999, 112:716–722
7. Satish L, Yager D, Wells A: ELR-negative CXC chemokine IP-9 as a mediator of epidermal-dermal communication during wound repair. *J Invest Dermatol* 2003, 120:1110–1117
8. Shiraha H, Gupta K, Glading A, Wells A: IP-10 inhibits epidermal growth factor-induced motility by decreasing epidermal growth factor receptor-mediated calpain activity. *J Cell Biol* 1999, 146:243–253
9. Bodnar RJ, Yates CC, Wells A: IP-10 blocks vascular endothelial growth factor-induced endothelial cell motility and tube formation via inhibition of calpain. *Circ Res* 2006, 98:617–625
10. Smith KD, Wells A, Lauffenburger DA: Multiple signaling pathways mediate compaction of the collagen matrices by EGF-stimulated fibroblasts. *Exp Cell Res* 2006, 312:1970–1982
11. Proost P, Schutyser E, Menten P, Struyf S, Wuyts A, Opendakker G, Dethoux M, Parmentier M, Durinx C, Lambey A-M, Neyts J, Liekens S, Maudgal PC, Billiau A, Van Damme J: Amino-terminal truncation of CXCR3 agonists impairs receptor signaling and lymphocyte chemotaxis, while preserving antiangiogenic properties. *Blood* 2001, 98:3554–3561
12. Satish L, Blair HC, Glading A, Wells A: IP-9 (CXCL11) induced cell motility in keratinocytes requires calcium flux-dependent activation of μ -calpain. *Mol Cell Biol* 2005, 25:1922–1941
13. Byrne C, Fuchs E: Probing keratinocyte and differentiation specificity of the human K5 promoter in vitro and in transgenic mice. *Mol Biol Cell* 1993, 13:3176–3190
14. Hebda PA, Whaley D, Kim H-G, Wells A: Absence of inhibition of cutaneous wound healing in mice by oral doxycycline. *Wound Repair Regen* 2003, 11:373–379
15. Greenhalgh DG: FACS: models of wound healing. *J Burn Care Rehab* 2005, 26:293–305
16. Fuchs E: Keratins and the skin. *Annu Rev Cell Dev Biol* 1995, 11:123–154
17. Boulday G, Haskova Z, Reinders MEJ, Pal S, Briscoe DM: Vascular endothelial growth factor-induced signaling pathways in endothelial cells that mediate overexpression of the chemokine IFN- γ -inducible protein of 10 kDa in vitro and in vivo. *J Immunol* 2006 Mar 1 176(5) 1; pp 3098–3107
18. Babu M, Wells A: Dermal-epidermal communication in wound healing. *Wounds* 2001, 13:183–189
19. Jinquan T, Quan S, Jacobi HH, Jing C, Millner A, Jensen B, Madsen HO, Ryder LP, Svejgaard A, Malling H-J, Skov PS, Poulsen LK: CXC chemokine receptor 3 expression on CD34+ hematopoietic progenitors from human cord blood induced by granulocyte-macrophage colony-stimulating factor: chemotaxis and adhesion induced by its ligands, interferon gamma-inducible protein 10 and monokine induced by interferon gamma. *Blood* 2000, 96:1230–1238
20. Lazzeri E, Romagnani P: CXCR3-binding chemokines: novel multifunctional therapeutic targets. *Curr Drug Targets Immune, Endocrine, Metabolic Disord* 2005, 5:109–118
21. Engelhardt E, Toksoy A, Goebeler M, Debus S, Brocker E-B, Gillitzer R: Chemokines IL-8, GRO α , MCP-1, IP-10, and Mig are sequentially and differentially expressed during phase-specific infiltration of leukocyte subsets in human wound healing. *Am J Pathol* 1998 Dec; 153(6); pp 1849–1860
22. Del Rio M, Larcher F, Meana A, Segovia JC, Alvarez A, Jorcano JL:

- Nonviral transfer of genes to pig primary keratinocytes. Induction of angiogenesis by composite grafts of modified keratinocytes overexpressing VEGF driven by a keratin promoter. *Gene Ther* 1999, 6:1734–1741
23. Tyner AL, Fuchs E: Evidence for posttranscriptional regulation of the keratins expressed during hyperproliferation and malignant transformation in human epidermis. *J Cell Biol* 1986, 103:1945–1955
 24. Shiraha H, Glading A, Chou J, Jia Z, Wells A: Activation of m-calpain (calpain II) by epidermal growth factor is limited by PKA phosphorylation of m-calpain. *Mol Cell Biol* 2002, 22:2716–2727
 25. Allen FD, Asnes CF, Chang P, Elson EL, Lauffenburger DA, Wells A: EGF-induced matrix contraction is modulated by calpain. *Wound Repair Regen* 2002, 10:67–76
 26. Gillitzer R, Goebeler M: Chemokines in cutaneous wound healing. *J Leukoc Biol* 2001, 69:513–521
 27. Flier J, Boorsma DM, vanBeek PJ, Nieboer C, Stoof TJ, Willemze R, Tensen CP: Differential expression of CXCR3 targeting chemokines CXCL10, CXCL9, and CXCL11 in different types of skin inflammation. *J Pathol* 2001, 194:398–405
 28. Hancock WW, Lu B, Gao W, Csizmadia V, Faia K, King JA, Smiley ST, Ling M, Gerard NP, Gerard C: Requirement of the chemokine receptor CXCR3 for acute allograft rejection. *J Exp Med* 2000, 192: 1515–1520